

## Correlated Ion Flux through Parallel Pores: Application to Channel Subconductance States

R.M. Berry and D.T. Edmonds

The Clarendon Laboratory, Oxford, OX1 3PU, UK

**Summary.** Many ion channels that normally gate fully open or shut have recently been observed occasionally to display well-defined subconductance states with conductances much less than those of the fully open channel. One model of this behavior is a channel consisting of several parallel pores with a strong correlation between the flux in each pore such that, normally, they all conduct together but, under special circumstances, the pores may transfer to a state in which only some of them conduct. This paper introduces a general technique for modeling correlated pores, and explores in detail by computer simulation a particular model based upon electric interaction between the pores. Correlation is obtained when the transient electric field of ions passing through the pores acts upon a common set of ionizable residues of the channel protein, causing transient changes in their effective pK and hence in their charged state. The computed properties of such a correlated parallel pore channel with single occupation of each pore are derived and compared to those predicted for a single pore that can contain more than one ion at a time and also to those predicted for a model pore with fluctuating barriers. Experiments that could distinguish between the present and previous models are listed.

**Key Words** multi-pore channel · correlated ion fluxes · subconductance states · channel model

### Introduction

The most frequently observed gating behavior of transmembrane ion channels is a simple switch between the two states, open and shut. However, many channels have recently been found to exhibit subconductance states with an ionic conductance less than that of the fully open state. Examples prior to 1987 may be found in the review by Fox (1987). Many recent reports concentrate on the calcium-activated potassium channel (Weik, Lonnendoker & Neumcke, 1989; Stockbridge, French & Man, 1991; Bezprozvanny, Benevolensky & Naumov, 1991; Lucchesi & Moczydlowski, 1991; Pottosin, 1992) but include examples of the inward rectifier (Matsuda, Matsuura & Noma, 1989), chloride channels (Schlichter et al., 1990), sodium channels

(Meves & Nagy 1989; Schreibmayer, Tritthart & Schindler, 1989; Ravindran, Schild & Moczydlowski, 1991) and calcium channels (Liu et al., 1989; Kunze & Ritchie, 1990; Kwok & Best, 1990). Models used to explain this behavior may be divided into two main types. The series models postulate a single pore that may undergo transitions to different configurations, leading to time-dependent changes in its conductance. The parallel models postulate a multi-barrel channel where the ion flow through parallel pores is normally correlated so that the pores all conduct or shut together, but where subconductance states are shown under particular circumstances when some pores close while others remain open. Experiments that favor the parallel model include observation of conductance levels that are integral multiples of a unit conductance (Miller, 1982; Krouse, Schneider & Gage, 1986; Hunter & Giebisch, 1987; Neumcke & Weik, 1988; Schreibmayer et al., 1989; Weik et al., 1989). Also, the finding that the subconductance states have the same ionic selectivity as the full conductance states (Hamill & Sakmann, 1981; Schreibmayer et al., 1989; Weik et al., 1989) is compatible with the series model only if the change in the pore configuration changes its conductance but not its selectivity. Less direct evidence is provided by channels which behave like several parallel pores that conduct independently (Miller, 1982; Krouse et al., 1986; Hunter & Giebisch, 1987) and thus show a binomial distribution of the total conductance. Such channels may resemble the channels discussed here in structure but may lack the apparatus required to correlate the ion flows.

Because the majority of ion channel transitions are between fully open and fully shut, the parallel model requires the ion flows to be strongly correlated. In this paper we briefly describe a general procedure for dealing with correlated ion flows through adjacent parallel pores and then describe in

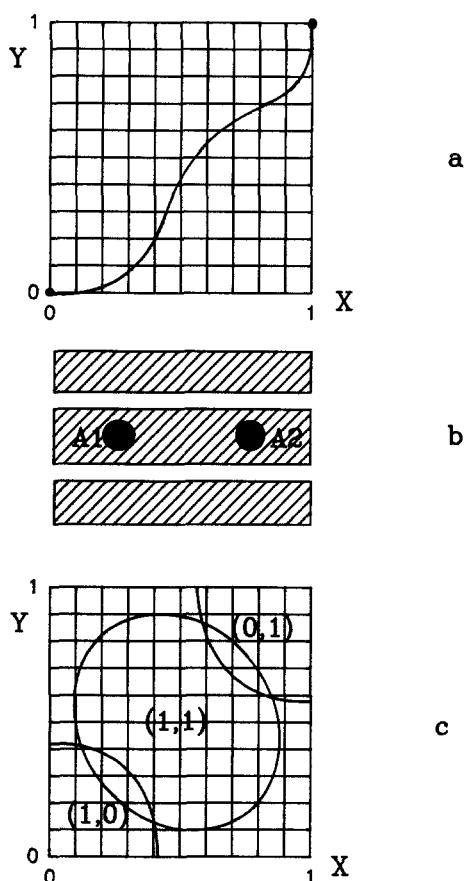


**Fig. 1.** (a) Map of the ion positions in the two parallel pores. The  $X$  and  $Y$  coordinates represent the ion positions within the first and second pore, respectively.  $X$  or  $Y = 0$  corresponds to an ion just outside the mouth of the pore on the left, while  $X$  or  $Y = 1$  corresponds to a position just out of the pore on the right. The line traces a possible trajectory of two ions crossing the membrane in a correlated fashion. (b) Sketch of two transmembrane pores with a pair of acid residues  $A1$  and  $A2$  between them. (c) Map of Fig. 1a showing contours within which the total energy,  $\langle U(X, Y) \rangle$  is small when the residues are in their charge states  $(1, 0)$ ,  $(1, 1)$  and  $(0, 1)$ . The contours are drawn at an energy 2 kT above that of the ground state of the system when no ions occupy the pores and the residues are uncharged.

more detail one physically plausible mechanism that could bring about the correlation. We show that if the ions passing through the parallel pores interact electrically with a common set of ionizable channel protein residues then the ion flows may become tightly coupled. The transient electric fields of the passing ions cause changes in the effective pK values of the ionizable residues which may lead to transient changes in their charge state (Edmonds, 1989). The electric fields of the residues in turn react upon the ions in the parallel pores controlling their flows. Computer simulations on a simple example of such a system demonstrate that correlated

parallel channels share some of the properties calculated (Hodgkin & Keynes, 1955; Hille & Schwarz, 1978) for multiply occupied single pores (which we will refer to as multi-ion pores), and also with pores with stochastically fluctuating barriers (Läuger, 1985). A list of the computed properties of correlated parallel pores is given together with experiments that could distinguish between the present model and previous ones.

### Theoretical Treatment of Correlated Parallel Pores

The general method is applied here to the simplest case of two parallel pores, but can be readily expanded to deal with any number. For the ion flows to be correlated, the channel protein containing the two pores must be capable of assuming different configurations, mechanical or electrical, to modulate the ion flows. The linear track of a single ion through a single pore is replaced by a two-dimensional map of ion positions in two parallel pores. We restrict the treatment to single occupation of each pore to ensure that any multi-ion effects observed are due to coupling between the pores, and not to interaction between ions in a single multi-ion pore. Such a map is shown in Fig. 1a, where the pair of coordinates  $(X, Y)$  defines the positions of an ion in the first and second pore, respectively.  $X$  or  $Y = 0$  indicates the ion is just out of the appropriate pore on the left, and  $X$  or  $Y = 1$  indicates the ion is just out of the channel on the right. As an example, the path shown by the heavy line represents first entry on the left of an ion into the first pore, followed by entry by an ion on the left into the second pore. The two ions make their way across the pores with the ion in the first pore leaving on the right followed by the ion in the second pore. Associated with every position  $(X, Y)$  on the map, representing the ion positions, we may plot along the  $Z$ -axis the total energy of the whole system of ions and channel,  $U(X, Y, N)$ , in each of the channel configurations labeled by  $N$ . An energy surface standing on the area  $0 < X < 1$ ,  $0 < Y < 1$  may thus be constructed for each different configuration  $N$ . Allowed transitions between the various energy states  $U(X, Y, N)$  of this system may be a change in  $N$  representing a change in the channel configuration without ion motion or a change in the  $X$  or  $Y$  coordinate at fixed  $N$  representing a change in an ion position. Having determined the values of  $U(X, Y, N)$ , statistical mechanics (Klein & Meijer, 1954) allows the calculation of the relative sizes of the thermally activated transition probabilities  $k_{ij}$  and  $k_{ji}$  between states with energies  $U_i$  and  $U_j$  using the relation

$$k_{ij}/k_{ji} = \exp(-U_j/kT)/\exp(-U_i/kT),$$

where  $k$  is the Boltzmann constant and  $T$  the absolute temperature. Given these transition probabilities, the evolution of the system in time consists of a thermally activated random walk between states along allowed paths. This may be simulated by computer using a Monte Carlo method. We have previously applied this technique to simulate the flow of ions through a single pore in a channel with electrical configurations that respond to the presence of ions within the pore (Edmonds, 1989; Edmonds & Berry, 1991; Berry & Edmonds, 1992).

The technique is much simplified if changes between the channel configurations are rapid in comparison with ion motion. In this case, associated with each ion position  $(X, Y)$ , we can replace the many values of  $U(X, Y, N)$  with a single "potential of mean force"  $\langle U(X, Y) \rangle$ , defined as the mean energy of the channel configurations weighted according to the probabilities of these configurations. This is equivalent to assuming that the channel configurations reach a quasi-equilibrium rapidly with the ions in a given position and in a shorter time than the mean time between ion movements. Then the progress of ions in the two parallel pores becomes simply a thermally activated random walk over this single energy surface  $\langle U(X, Y) \rangle$ . In the particular example we will explore in detail, the channel configurations consist simply of the four possible charge states of two ionizable residues which interact with ions in the pores. Correlated parallel ion flows in the two channels are represented by diagonal paths on the map in Fig. 1a, and configuration energies must encourage such paths if correlated ion flow is to be observed.

#### A SIMPLE ELECTRIC MODEL OF CORRELATED PARALLEL PORES

The simplest model that exhibits the desired characteristics is sketched in Fig. 1b. The channel consists of two identical narrow pores interacting with the same two ionizable acid residues A1 and A2. The charged states of the residues may be labeled (1, 0) if only the left residue is negatively charged, (0, 1) if the right residues is charged and (1, 1) and (0, 0) if both or neither are charged. We have previously described (Edmonds & Berry, 1991) how such a pore may be made selective to cations within a narrow range of unhydrated radius by adjusting the distance of the acid residues from the pore. We will assume here that both pores are selective to  $K^+$  ions. Because the pores are assumed to be narrow, the ions within them are only partially hydrated and a large energy barrier (Parsegian, 1969) faces a  $K^+$  ion attempting to enter either pore with the channel in its uncharged state (0, 0). In the state (1, 0), the

electrostatic interaction with the negatively charged left-hand residue lowers this barrier on the left and thus allows easy entry for  $K^+$  ions from the left. The remaining barrier on the right prevents further transfer of the ions to the right. Similarly, the state (0, 1) allows easy entry from the right but no through passage. In the state (1, 1) ions towards the middle section of each pore can interact favorably with both charged residues. However, the repulsion between the two charged residues raises the energy of the whole configuration in this state so that, only when both ions are near the middle of each pore, is the total energy low. The similarity in ion access between the states (1, 0) and (0, 1) and a binding cavity open to the left side and the right side, respectively; and the similarity between the state (1, 1) and an occluded cavity, explains why charge-responsive channels have some properties in common with carrier models (Berry & Edmonds, 1992). The energy profile along each pore in the four charged states has been recently described in some detail in the papers dealing with single pores referred to in the Introduction.

Not only does the charge state of the residues determine the energy profile seen by a  $K^+$  ion moving through a pore, but the ion positions within the pores determine also which charge state of the residues is probable. Thus, for example, cations at the left-hand end of a pore help to lower the energy of, and hence stabilize, the charge state (1, 0). In a real sense, cations within a pore help change the charge state of the residues to that which aids further progress through the pore. Figure 1c maps the ion positions within the pores; the contours drawn on top show the regions within which the charge states (1, 0), (0, 1) and (1, 1) have low energy and are thus likely to occur. As can be seen, coupled motion of a pair of cations from left to right, corresponding to a diagonal path on the map, can be encouraged if accompanied by cyclical changes in the residue charge states in the sequence (1, 0), (1, 1) (0, 1).

To simplify the computer simulation, the path of an ion in each pore is replaced by five equally separated steps so that the map of Fig. 1a becomes a grid of 25 positional states. The evolution of the system is then determined using a Monte Carlo method described in full elsewhere (Berry & Edmonds, 1992). The energies  $U(X, Y, N)$  were calculated by representing the membrane as a homogeneous slab of a relative dielectric constant of 2.4 and thickness of 20 Å, surrounded by aqueous fluid of dielectric constant 80. The ionizable residues were placed 6 Å from the membrane surfaces and the axes of the parallel pores are separated by 12 Å. All interactions were then calculated using the method of images (Neumcke & Lauger, 1969). Such calcula-

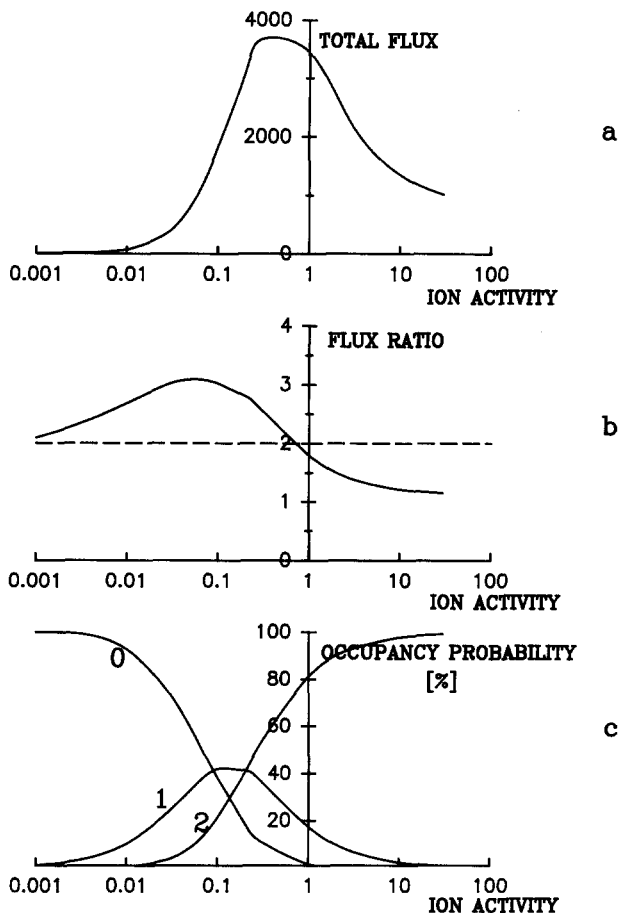


**Fig. 2.** (a) Net ion flux left to right through the two-pore channel as a function of the absolute ion activity on the right when no voltage is applied and the ion activity on the left is always twice that on the right. The flux is shown as ions per  $10^6$  time units, where one time unit is the average time for a single ion to take a single step within a pore. (b) Ratio of the unidirectional fluxes under the same conditions that prevail in a. The broken line gives the Ussing ratio predicted for independent motion of the ions. (c) The curves marked 0, 1 or 2 give the time-averaged percentage probabilities that the two-pore channel is occupied by 0, 1 or 2 ions as a function of the absolute ion activity on the right as in a or b.

tions are unlikely to be accurate but this procedure does impose a relative consistency on the interaction energies used. The model, in fact, does not depend strongly on the energies calculated. As is usual in such calculations, we used absolute ionic activities of the fluids bathing the two faces of the membrane which give the number of ions available for entry and defined them as the number by which the probability of entry is multiplied to obtain the mean entry rate. The pK values of the two acid sites are assumed to be 8, corresponding possibly to a glutamic acid residue with its pK raised by 3 units due to the low electrical polarizability of its environment within the membrane (Edmonds, 1989).

## Results

Figure 2a shows the calculated, total net, left-to-right flux through the combined two-pore channel as a function of ion activity at the right-hand end of the pores when no voltage is applied across the membrane, but the ion activity on the left is twice that on the right. The steep rise of the net flux as a function of ion activity, which is a unique feature of this model, reaches a maximum when the flux becomes proportional to [activity]<sup>1.51</sup>. As the ion concentration increases further, the net flux saturates and finally falls. If the pores acted independently, we would expect a maximum ratio of the unidirectional fluxes of 2, which is the Ussing ratio for a 2:1 ratio of the ionic activities. As seen in Fig. 2b, however, much higher ratios are calculated in the medium range of activities. This indicates positive coupling between the fluxes, and has traditionally been taken as evidence of multiply occupied pores. Furthermore, these high ratios occur at lower concentrations than with traditional multi-occupancy models, where they are only seen at concentrations near saturation when multiple occupancy of a single pore becomes probable.

A new type of behavior is seen at very high activities. In this limit, it is unlikely that the channel will ever be empty. After the exit of the first ion on the right, following a coupled left-to-right transit of the membrane by a pair of ions, the channel is held in the (0, 1) state by the remaining ion. While this state persists, another ion may only enter from the right. This leads to behavior like a 1:1 shuttle, resulting in a ratio of the unidirectional fluxes of 1, below the Ussing ratio of 2 for a 2:1 concentration gradient. Such behavior clearly distinguishes this type of model from multi-ion pore models where the unidirectional flux ratio may never drop below the Ussing ratio. This carrier-like mode has been fully described for a single channel in a recent paper (Berry & Edmonds, 1992) and will not be further discussed here. Figure 2c shows the probability of zero, one or two ions occupying the two-pore channel as a function of the ion activity on the right, as above. The model predicts that both the flux and unidirectional flux ratio will rise to a maximum and then fall as the pH is decreased from an initial high value. This is to be expected as the charged state of the sites depends upon (pK - pH) and extreme values of pH will remove (pK - pH) from the range, where the shifts in pK brought about by the electric fields of transient ions result in changes in the charged states of the sites. The traditional multi-occupancy models do not explicitly depend upon pH.

Some of the observations of subconductance states referred to in the Introduction only occur in

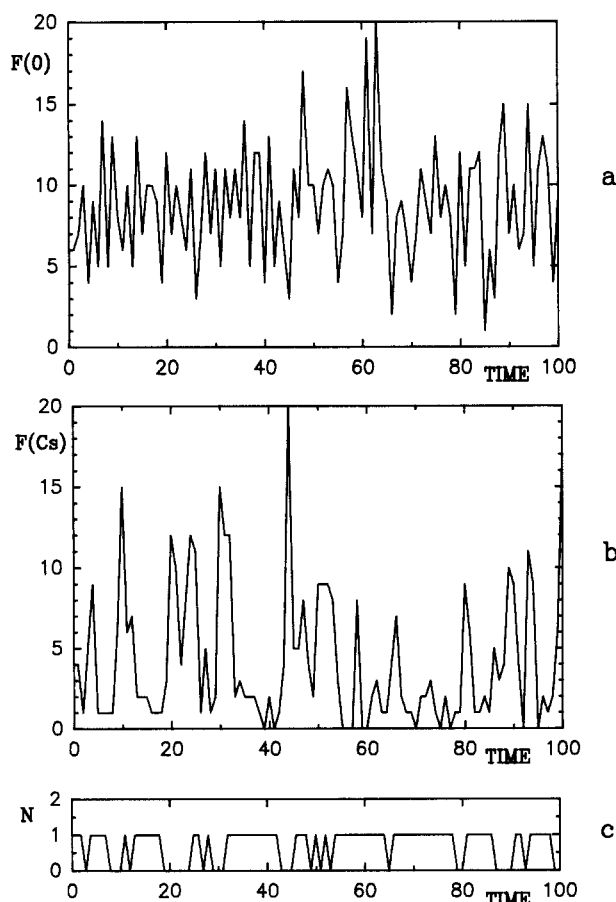


**Fig. 3.**  $K^+$  flux as a function of time calculated for 100 successive intervals of  $10^4$  of the time units defined for Fig. 2b, with a  $K^+$  ion activity of 0.03 on both sides and a transmembrane voltage of 100 mV applied. (b)  $K^+$  flux as in *a* after  $Cs^+$  ions, which block the pores, are introduced with an activity of 0.001 on the left only. (c) Occupancy of the two pores by  $Cs^+$  ions at the end of each period. Comparison of *a*, *b*, and *c* reveals that the channel has its full conductance when no  $Cs^+$  ion is present within either pore, but that the presence of  $Cs^+$  in either pore reduces the conductance of the channel to a value much less than half the conductance in the absence of  $Cs^+$  ions.

the presence of a small concentration of a second ion such as  $Cs^+$  or  $Ba^{2+}$ , which is thought to bind strongly to or block individual pores. To demonstrate this type of behavior in the two-pore channel, the model was adapted to allow a second type of ion—which we shall arbitrarily call  $Cs^+$ —to enter both pores. For simplicity, energy profiles for  $Cs^+$  are the same as those for  $K^+$ , except for a barrier preventing  $Cs^+$  ions leaving at the right-hand end of the pores. The number of  $K^+$  ions passing through the two pores during each period of  $10^4$  time intervals is plotted in Fig. 3a for 100 such periods, showing the normal current shot noise when the  $K^+$  ion activity is 0.03 on both sides and a transmembrane voltage of 100 mV is applied. If  $Cs^+$  ions are now

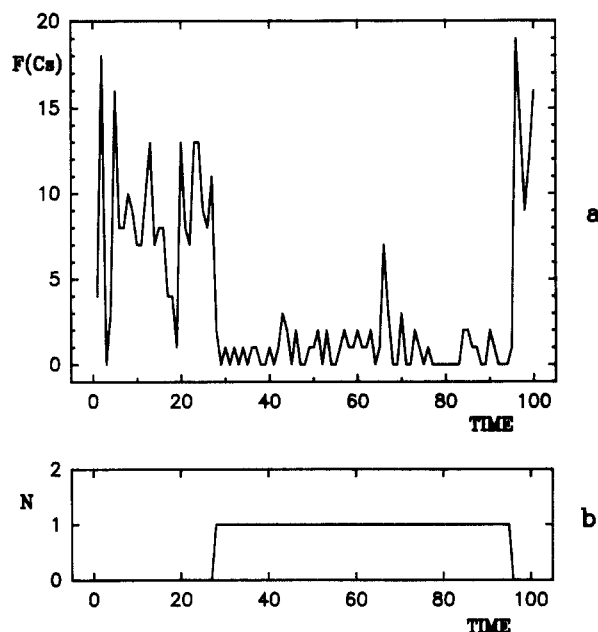


**Fig. 4.** (a)  $K^+$  flux in the presence of  $Cs^+$  as in Fig. 3b, but with the rate constant for  $Cs^+$  reduced by a factor of 10. (b) Occupancy of the two pores by  $Cs^+$  ions. Comparison of *a* and *b* shows that while a  $Cs^+$  ion occupies one pore, the conductance of the second pore is much reduced.

added at the left with an activity of 0.001, the  $K^+$  ion flux becomes that shown in Fig. 3b. The number of  $Cs^+$  ions occupying the pores at the end of each time interval is shown in Fig. 3c. Comparison between Fig. 3b and *c* reveals that when no  $Cs^+$  ion occupies the pores, the channel has its full conductance, but when a single  $Cs^+$  ion enters either pore, a subconductance state exists with a conductance much less than half the full conductance. In the simulation shown in Fig. 3, the time taken for a  $Cs^+$  ion to enter and leave is comparable to the transit time of a  $K^+$  ion and is so fast that it makes the two conductance states hard to resolve. The transitions between the two conductance states add to the low frequency noise of the ion current—a situation often referred to as a “flickering block.” The nature of the subconductance state is more clearly seen in simulations in which the rate constant used to compute the motion of the  $Cs^+$  ion is reduced by a factor of 10 in comparison with that used for the majority of  $K^+$  ions. This situation is illustrated in Fig. 4, where two distinct average rates of transfer are seen in Fig. 4a, corresponding to whether one pore is occupied by a  $Cs^+$  ion as indicated in Fig. 4b. These simulations demonstrate that a channel consisting of two parallel pores with one blocked by a nonpermeant ion may exhibit a subconductance state with a conductivity anywhere between that of a single pore and zero, depending on the strength of the

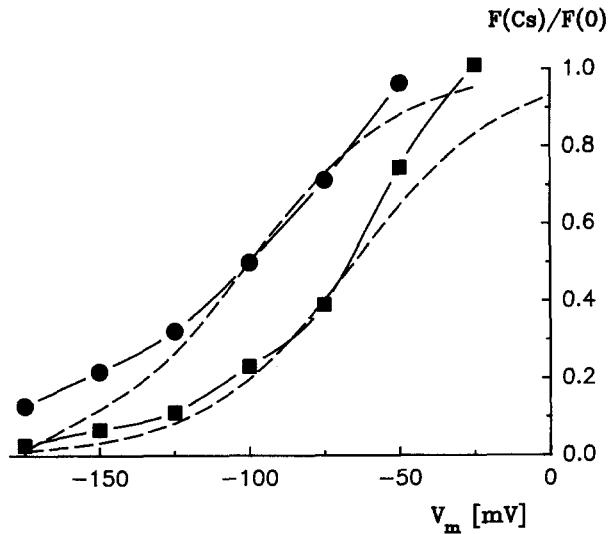


**Fig. 5.** Ratio of the flux of  $K^+$  ions in the presence of blocking  $Cs^+$  ions  $F(Cs)$ , to that in the absence of  $Cs^+$  ions  $F(0)$  plotted as a function of the left-to-right transmembrane voltage.  $K^+$  activity is always 0.03 on both sides and the full lines marked by filled circles and filled squares correspond to  $Cs^+$  activities of 0.001 and 0.01, respectively. The broken lines give the corresponding fluxes expected with no coupling between the two pores, normalized to be the same in each case when  $F(Cs)/F(0) = 0.5$ .

coupling between the two pores. Thus, the finding of channel subconductance levels that are not simply submultiples of the full conductance is not an argument against the parallel model.

Figure 5 shows the ratio of the left-to-right flux of  $K^+$  in the presence of  $Cs^+$  to that without  $Cs^+$  as a function of the left-to-right transmembrane voltage.  $K^+$  is present on both sides with an absolute activity of 0.03, while  $Cs^+$  is present only on the left at absolute activities of 0.001 (●) and 0.01 (■). For comparison, the dotted lines show the fluxes expected if the blockage were by the  $Cs^+$  ions in independent channels. The steepness of the voltage dependence indicates that more than one ion moves in the formation of the blocked states. This behavior, due to coupling between two single-occupancy pores, is also seen in the multi-ion pore model (Hille & Schwarz, 1978).

One way of describing parallel pores with correlated ion fluxes is an ion/ion coport in which the two ions are of the same type. To illustrate this coport nature, a simulation was performed in which one of the pores is made selective only to type A ions and the other only to type B ions. In these circumstances, it is possible to illustrate clearly the coupling of the two types of ion flow. It is also possible to show how type A ions moving down their electrochemical potential gradient within their pore can drive type B ions within their pore in the

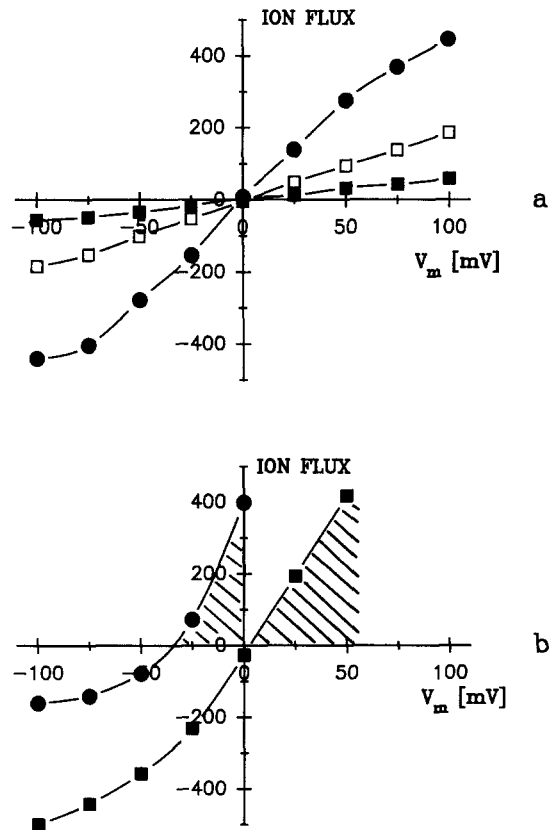


**Fig. 6.** The two-pore channel acting as an ion/ion coport. (a) The full line marked with filled circles gives the average flux of either A or B type ions in  $10^4$  time units as a function of transmembrane voltage when both types are present at both sides with absolute activities of 0.03. The open squares show the flux of type A ions when the A ion activity remains at 0.03 at both sides, but that of the B type ions is reduced to 0.003 on both sides. The marked reduction in the flux of A type ions is due to the coupling between the two pores. The filled squares give the simultaneous flux of the B type ions at their reduced activity. (b) The line with filled circles gives the voltage dependence of the left-to-right flux of B type ions with activities of 0.03 at both sides of the membrane when driven by coupling between the pores and the A type ions have left and right activities of 0.3 and 0.003, respectively. The shaded area shows the region in which the flux of B ions has been converted from negative to positive by the inter-pore coupling. The line marked by filled squares gives similar information for type B ions that have left and right activities of 0.01 and 0.1, respectively, tending to oppose the flow driven by coupling to the A ions in the other pore.

same direction but against their electrochemical potential gradient, as required of a coport. We have previously demonstrated a single pore ion/proton counterport working on similar principles (Edmonds & Berry, 1991). The filled circles in Fig. 6a show the left-to-right flux of type A or type B ions through the two-pore channel as a function of the transmembrane voltage when the ions are present with absolute activity of 0.03 on both sides of the

membrane. The open and filled squares show the flux of type A and type B ions, respectively, when the activity of the type A ions remains the same but that of type B is reduced by a factor of 10 to 0.003. The marked reduction of the flux of type A ions when their activity remains unchanged demonstrates the coupling of the ion flows in the two pores. The filled circles in Fig. 6b show the flux of type B ions with an activity of 0.03 at each side when driven by a 100:1 left-to-right activity ratio of type A ions. The hatched area under the curve shows the region in which the flux of type B ions is switched from negative to positive by the driving force of the type A ionic gradient. The filled squares show a situation with the same driving gradient of type A ions but in which the type B ions now face an adverse right-to-left activity ratio of 10:1.

#### POSSIBLE EXPERIMENTAL TESTS OF THE MODEL

The predicted properties of the correlated two-pore model are listed below. They are compared to those predicted for multi-ion channel models (Hodgkin & Keynes, 1955; Hille & Schwarz, 1978) or those predicted by models of single pores with fluctuating barriers (Läuger, 1985). To distinguish between ion interactions within a single pore and those in parallel pores, we have assumed throughout single occupancy of each of the parallel pores. A real multi-barrel channel may allow more than one ion in each pore and would tend to blur the clear distinctions we make between the two types of model. Experiments which could distinguish between the different types of model are suggested.

#### (1) Concentration Dependence of Ionic Flux

With the parallel model, ionic fluxes through the channel rise to a maximum and then fall (Fig. 2a) as the ion activity rises. At low activities the dependence is superlinear, with flux proportional to the activity raised to a power greater than 1. Both multi-occupancy and fluctuating barrier models also predict a maximum in flux *vs.* activity, but neither predicts superlinear dependence at any activity. The two-pore model could be tested by studying the dependence of flux on ionic concentration at low concentrations.

#### (2) Unidirectional Flux Ratios

In the parallel model, the unidirectional flux ratio rises above the Ussing ratio at low and medium activities, but at very high activities it can fall well

below the Ussing ratio to approach the value 1 usually associated with a 1:1 carrier (Fig. 2b). Multi-ion models predict flux ratios equal to or above the Ussing ratio, while fluctuating barrier models predict flux ratios equal to or below the Ussing ratio. Experiments with radioactive tracer ions at approximately physiological concentrations (Vestergaard-Bogind, Stampe & Christopherson, 1985) find flux ratios larger than the Ussing ratio. Extending such experiments to higher ionic concentrations would test the carrier-like nature of the two-pore channel at high ion activities.

#### (3) Partial Channel Block by Additional Impermeable Ions

Subconductance states are observed (Figs. 3b and 4a) in the presence of a small concentration of a second impermeant ion. The conductance of the remaining unblocked parallel pores may range from totally unblocked to totally blocked, depending on the strength of the correlation between pores. The observation of subconductance states with conductances that are not an integer submultiple of the full conductance are thus consistent with a partially blocked multi-barrel channel. The voltage dependence of the blockage (Fig. 5) is steeper than would be expected with uncorrelated pores.

#### (4) Streaming Potential

The streaming potential is the transmembrane voltage resulting from an osmotic pressure gradient, and it may be related to the number of ions carried through a pore in single file with water molecules (Levitt, 1984). Measurement of the streaming potential through gramicidin channels shows that the number of ions in this narrow pore increases with the ion concentration within the same range that the flux ratio increases. This will not be the case in correlated parallel pores where the high flux ratios are due to coupling between ions in different, singly occupied pores. Streaming potential measurements on calcium-activated  $K^+$  channels (Pottosin, 1992) do provide some evidence in favor of the parallel pore model.

#### Discussion

We have shown that correlation of the ion flows through identical parallel pores may result simply from the electrical interaction between the transient ions and a common set of ionizable residues of the

channel protein. The correlation results in anomalous, multi-ion effects due to coupling between ions in adjacent, singly occupied pores rather than the interaction of several ions within the same pore. Correlated ion fluxes are required by the parallel models of ion channels, which exhibit subconductance states referred to in the Introduction. The known oligomeric structure of many channels, including the potassium channel, and the ability to form conducting potassium channels from heterooligomers derived from mixed mRNA's (Miller, 1991), is consistent with the subunits providing parallel pores and the common central region providing the correlation and gating. Multi-ion effects, which are such a feature of many potassium channels, could then be due, at least in part, to the correlation of ion fluxes in the parallel pores of the channel.

R.M.B. is grateful to the S.E.R.C. for the award of a graduate studentship.

## References

- Berry, R.M., Edmonds D.T. 1992. Carrier-like behaviour from a static but electrically responsive model pore. *J. Theoret. Biol.* **154**:249–260
- Besprozvanny, I.B., Benevolensky, D.S., Naumov, A.P., 1991. Potassium channels in aortic microsomes: conductance, selectivity, barium induced blockage and subconductance states. *Biochim. Biophys. Acta* **1064**:75–80
- Edmonds, D.T. 1989. A kinetic role for ionizable sites in membrane channel proteins. *Eur. Biophys. J.* **17**:113–119
- Edmonds, D.T., Berry, R.M. 1991. The proton ladder, a static mechanism for ion/proton coports and counterports. *Eur. Biophys. J.* **20**:241–245
- Fox, J.A. 1987. Ion channel subconductance states. *J. Membrane Biol.* **97**:1–8
- Hamill, O.P., Sakmann, B. 1981. Multiple conductance states of single acetylcholine receptor channels in embryonic muscle cells. *Nature* **294**:462–464
- Hille, B., Schwarz, W. 1978. Potassium channels as multi-ion single-file pores. *J. Gen. Physiol.* **72**:409–442
- Hodgkin, A.L., Keynes, R.D. 1955. The potassium permeability of a giant nerve fibre. *J. Physiol.* **128**:61–68
- Hunter, M., Giebisch, G. 1987. Multi-barreled K channels in renal tubules. *Nature* **327**:522–524
- Klein, J.K., Meijer, P.H.E. 1954. Principle of minimum entropy production. *Phys. Rev.* **96**:250–255
- Krouse, M.E., Schneider, G.T., Gage, P.W. 1986. A large anion-selective channel has seven conductance levels. *Nature* **319**:58–60
- Kunze, D.L., Ritchie, A.K. 1990. The DHP-sensitive calcium channel in GH<sub>3</sub> cells exhibits multiple conductance levels. *Biophys. J.* **57**:396a
- Kwok, W.M., Best, P.M. 1990. Ryanodine sensitivity and multiple conductance states of the Ca release channel from native SR membrane. *Biophys. J.* **57**:168a
- Läuger, P. 1985. Ion channels with conformational substates. *Biophys. J.* **47**:581–591
- Levitt, D.G. 1984. Kinetics of movement in narrow channels. *Curr. Top. Membr. Transp.* **21**:181–197
- Liu, Q.Y., Meissner, G., Lai, F.A., Rousseau, E., Jones, R.V. 1989. Multiple conductance states of the purified calcium release channel complex from skeletal sarcoplasmic reticulum. *Biophys. J.* **55**:415–424
- Lucchesi, K.J., Moczydlowski, E. 1991. On the interaction of bovine pancreatic trypsin inhibitor with maxi Ca<sup>2+</sup>-activated K<sup>+</sup> channels. *J. Gen. Physiol.* **97**:1295–1319
- Matsuda, H., Matsuura, H., Noma, A. 1989. Triple barrel structure of inwardly rectifying K<sup>+</sup> channels revealed by Cs<sup>+</sup> and Rb<sup>+</sup> block in guinea-pig heart cells. *J. Physiol.* **413**:139–157
- Meves, H., Nagy, N. 1989. Multiple conductance states of the sodium channel and of other ion channels. *Biochim. Biophys. Acta* **988**:99–105
- Miller, C. 1982. Open-state structure of single chloride channels from *Torpedo* electroplax. *Philos. Trans. R. Soc. B* **299**:401–411
- Miller, C. 1991. *Annus mirabilis* of potassium channels. *Science* **252**:1092–1096
- Neumcke, B., Läuger, P. 1969. Nonlinear electrical effects in lipid bilayer membranes. *Biophys. J.* **9**:1160–1170
- Neumcke, B., Weik, R. 1988. Subconductance states of K channels in mouse muscle. *Pfluegers Arch.* **412** (Suppl. No. 1):R14
- Parsegian, V.A.Q. 1969. Energy of an ion crossing a low dielectric membrane: solutions of four relevant problems. *Nature* **221**:844–846
- Pottosin, I.I. 1992. Probing of pore in the *Chara* gymnomphylla K<sup>+</sup> channel by blocking cations and by streaming potential measurements. *FEBS Lett.* **298**:253–256
- Ravindran, A., Schild, L., Moczydlowski, E. 1991. Divalent cation selectivity for external block of voltage dependent Na<sup>+</sup> channels prolonged by Batrachotoxin. *J. Gen. Physiol.* **97**:89–143
- Schlichter, L.C., Grygorczyk, R., Pahapill, P.A., Grygorczyk, C. 1990. A large multiple-conductance chloride channel in normal human T-lymphocytes. *Pfluegers Arch.* **416**:413–421
- Schreibmayer, W., Tritthart, H.A., Schindler, H. 1989. The cardiac sodium channel shows a regular substate pattern indicating synchronized activity of several ion pathways instead of one. *Biochim. Biophys. Acta* **986**:172–186
- Stockbridge, L.L., French, A.S., Man, S.F.P. 1991. Subconductance states in calcium-activated potassium channels from canine airway smooth muscle. *Biochim. Biophys. Acta* **1064**:212–218
- Vestergaard-Bogind, B., Stampe, P., Christopherson, P. 1985. Single-file diffusion through the Ca<sup>2+</sup>-activated K<sup>+</sup> channel of human red cells. *J. Membrane Biol.* **88**:67–75
- Weik, R., Lonnendonker, U., Neumcke, B. 1989. Low-conductance states of K<sup>+</sup> channels in adult mouse skeletal muscle. *Biochim. Biophys. Acta* **983**:127–134

Received 31 July 1992; revised 18 November 1992